Kufa Journal of Engineering
Vol. 16, No. 1, January 2025, P.P. 104-120
Article history: Received 20 April 2024, last revised 13 June 2024, accepted 5 July 2024

PID CONTROLLER FOR SPEED CONTROL OF PMSM BASED ON MAYFLY OPTIMIZATION ALGORITHM

Fatimah F. Jaber

Assistant lecturer at Electrical Engineering Techniques Department, Engineering Technical College/Basra, Southern Technical University,Iraq,
Email: Fatimah.jaber@stu.edu.iq.

https://doi.org/10.30572/2018/KJE/160107

ABSTRACT

Permanent magnet synchronous motor (PMSM) is extensively employed in AC servo drives owing to their superior torque-to-inertia ratio, power density, efficiency, and power factor compared to other motors. So, it is a crucial point to regulate the PMSM speed. Conventional proportional, integral, and differential (PID) is a simple controller and easy to implement but it is coefficients are essentially determined by experience when used in PMSM to control the speed. This invariably produces unacceptable outcomes, in addition when it comes to low-power application drives, PID controller gains typically produce adequate results but, when it comes to high-power application drives, an untuned PID does not deliver satisfactory performance. The optimization algorithm offers an effective method to produce optimal PID gains. Therefore, to optimize the PID coefficients to regulate the PMSM speed, this study suggests a mayfly optimization algorithm (MA). Recently, the MA was introduced as a new intelligent optimization method with exceptional optimization capabilities. Nuptial dancing and random flight improve the ability of the algorithm to balance its features of exploitation and exploration while assisting in its escape from local optima. This suggested approach has been verified with MATLAB, and the outcomes are compared with the standard particle swarm optimization technique (PSO) and conventional PID. The outcomes show that compared to the standard PSO or conventional PID, the PID parameters adjusted by the MA method can produce faster speed responses and less overshoot. Furthermore, the system's optimal ITAE index value, as determined by the MA technique, is smaller (0.794) as compared to other techniques 1.503 and 1.906 respectively.

KEYWORDS

PID, PMSM, Mayfly, MATLAB, PSO.

1. INTRODUCTION

The PMSM is now broadly acknowledged as a prominent drive technology in industrial applications, such as robots, electric cars, and aircraft. The Permanent magnet synchronous motor model is a complex non-linear system with multiple inputs and outputs that can be affected by both parametric errors and shocks (Orlowska-Kowalska et al., 2022, Cervone et al., 2021). As a result, researchers both domestically and internationally are very interested in stability control (Deng et al., 2019, Ren et al., 2021), such as using sliding mode control. In this study (Junejo et al., 2020), to enhance the speed control performance of a Permanent magnet synchronous motor with external and internal disruptions, a new ATSMRL (adaptive terminal sliding mode reaching law) with CFTSMC (continuous fast terminal sliding mode control) is introduced. Comprehensive numerical and experimental investigations were performed to show that the ATSMRL approach outperformed the TSMRL (terminal sliding mode reaching law) and the ESMRL (standard exponential sliding mode reaching law). A well-liked and useful method that makes motors more responsive to abrupt changes and stabilizes motor current is the model predictive current controller (Liu et al., 2022). A classic nonlinear control system is the PMSM; it is challenging to achieve good control performance with traditional PI control. As a result, several new control techniques are suggested and used with PMSM, such as model predictive control (MPC), MPC outperforms FOC dynamically, but since it lacks modulation units, it performs poorly in the steady state. In this work (Zhang et al., 2020), Aside from the main vectors of the voltage of an inverter, virtual vectors can be produced using the DSVM (discrete space vector modulation) method. DSVM-based MPC helps eliminate current harmonics and torque ripples in a PMSM drive. However, a high number of candidate voltage vectors also considerably increases the computing burden. Therefore, a unique DSVM-based MPC is proposed in this paper. It can efficiently calculate three-phase duty ratios and choose the best voltage vector without listing every candidate voltage vector, resulting in a good performance with minimal computing burden. In (Sun et al., 2021), An improved MPCC method for the PMSHM (permanent magnet synchronous hub motor) drives is presented in this work. (Sun et al., 2021), This work proposes a novel FCS-MPCC that combines duty cycle control and a virtual vectors expansion approach to drive PMSHMs without the need for a modulator.

Using a PID controller is a popular control technique for PMSM speed control. PID's straightforward design, straightforward underlying idea, and numerous other benefits make it well-liked in different industrial control domains. However, empirical trial and error is typically the only way to estimate the three PID parameters (proportional (K_p), integral (K_i), and differential (K_d)). The chosen parameters may not be the best option, which will unavoidably cause issues with the control mechanism including poor stability and sluggish response speed. In tandem with the ongoing advancements in computer and control technologies, scholars are expanding their investigation into PID parameter-setting techniques. In this work (Jin et al., 2020, Teymoori et al., 2023), employed traditional fuzzy control PID to produce favorable outcomes. In (Ahmed et al., 2021), a FOPID (Fractional order proportional, integral, and derivative) controlling is used in this PMSM derive system under study to implement the current and speed controllers. The application of population optimization methods is becoming increasingly prominent among the many optimization techniques for the PID. Most population optimization methods don't depend on how accurate the system equations of the optimization system are, and they improve in accuracy over time by continuously updating different parameters and producing satisfying results in a variety of sectors. The PID controller in this study (Jamil and Moghavvemi, 2021) will be adjusted using a variety of techniques, including evolutionary algorithms like PSO and Genetic Algorithm (GA), and heuristic techniques like Trial and Error (T&E) and Ziegler Nichols (ZN). The simulations demonstrate that the PSO and Genetic Algorithm outperform TE and ZN techniques. On the other hand, the PSO outperformed the GA in terms of optimizing the PID constants more quickly. However, Global optimization cannot be effectively performed by typical GA techniques. In (Chen et al., 2022), For improved compensation performance, the GAPSO algorithm optimizes the parameters of the FOPID. It is dependent upon GA and PSO techniques. In this work (Wu et al., 2020), to preserve system stability as much as feasible, the PSO method was enhanced to adaptively alter the algorithm's weight. Even if the stability speed increased, the algorithm's improvement was too simple, making it difficult to jump if one became stuck in a local optimum.

A newly developed intelligent optimization technique is the MA optimization algorithm. Furthermore, the algorithm draws inspiration from the mating process and the flight behavior of mayflies, which includes random strolling, group gatherings, wedding dances, and mayfly crossings. Additionally, the method combines the primary benefits of evolutionary algorithms and swarm intelligence. The Mayfly optimization algorithm has garnered significant interest due to its unique benefits in terms of speed, exploitation, and convergence precision (Bhattacharyya et al., 2020, Amudha et al., 2021). The PMSM's regulation quality and stable operation are directly impacted by the PID controller's parameters (Injeti and Divyavathi, 2019). Consequently, it is essential to choose the three parameters of PID ($K_p, K_i, and\ K_d$) correctly to enhance the system's dynamic quality. Given the aforementioned information, a mayfly optimization technique is presented in this study and used to optimize the PMSM's PID parameters, and comparative simulations are conducted with alternative optimization techniques to confirm the MA algorithm efficiency.

2. MODEL OF THE PMSM SYSTEM

Maximum torque current ratio control and $i_d = 0$ control is currently the most commonly utilized technique in classic vector control (Huang et al., 2021, Liang et al., 2014, Lin et al., 2018). Fig. 1 depicts the control block design for the $3-\phi$ PMSM is used in this work. The synchronous rotating coordinate axis, d,q serves as the foundation for the mathematical model of the $3-\phi$ permanent magnet synchronous motor was chosen for this study. The equation of stator voltage in the d-q coordinate is (Thike and Pillay, 2020, Wang et al., 2020):

$$u_d = Ri_d + L_d \frac{di_d}{dt} - \omega_e L_q i_q \quad (1)$$

$$u_q = Ri_q + L_q \frac{di_q}{dt} - \omega_e (\psi_f + L_d i_d) \quad (2)$$

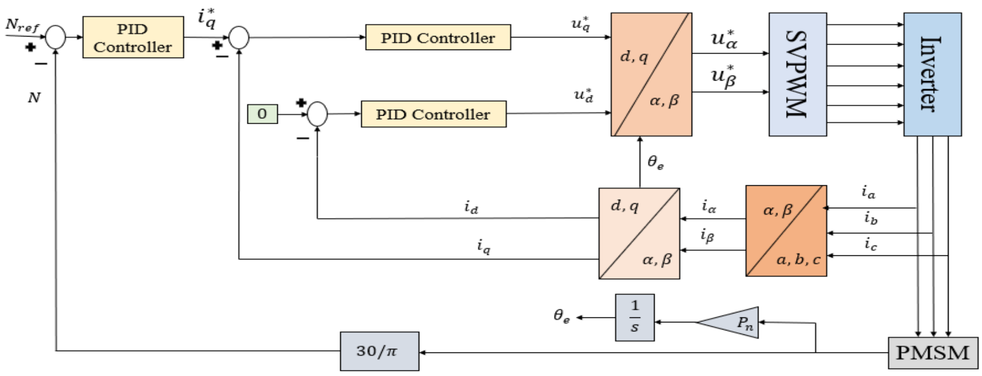

Fig. 1. Block schematic representation for the vector control of the $3-\phi$ PMSM

Where the d-axis, q-axis voltages of the stator, q-axis, and d-axis currents in the d-q coordinate of the synchronous rotation axis are represented by the variables u_d, u_q, i_q, and i_d, respectively. The permanent magnet flux is represented by ψ_f, the electrical angular velocity by ω_e, the resistance of the stator by R, and the q, d-axis inductance components of the motor by L_q *and* L_d respectively(Guo et al., 2022). To tune PID as a speed controller, the three-phase PMSM's motor motion equation is recast as follows:

$$J\frac{d\omega}{dt} = T_e - T_L - B\omega_m \quad (3)$$

$$T_e = \frac{3}{2} P_n i_q [i_d(L_d - L_q) + \psi_f] \quad (4)$$

In equations (3), ω_m represents the mechanical angular speed, T_e is the electromagnetic torque, the moment of inertia is represented by J, T_L denotes the load torque, while B represents the damping coefficient, and P_n is the pole pair.

The conventional PID controller is described below:

$$u(t) = K_p\, e(t) + K_i \int_0^t e(t)dt + K_d \frac{de(t)}{dt} \tag{5}$$

The PID controller's transfer function is described below:

$$G(s) = K_p + K_i \frac{1}{s} + K_d\, s \tag{6}$$

As a result, the PID controller's speed-loop controller expression is (Ortega et al., 2002):

$$i_q^* = (K_p + K_i \frac{1}{s} + K_d\, s) * (\omega_m^* - \omega_m) - B_a \omega_m \tag{7}$$

Fig. 2 displays the entire Simulink model for the suggested approach.

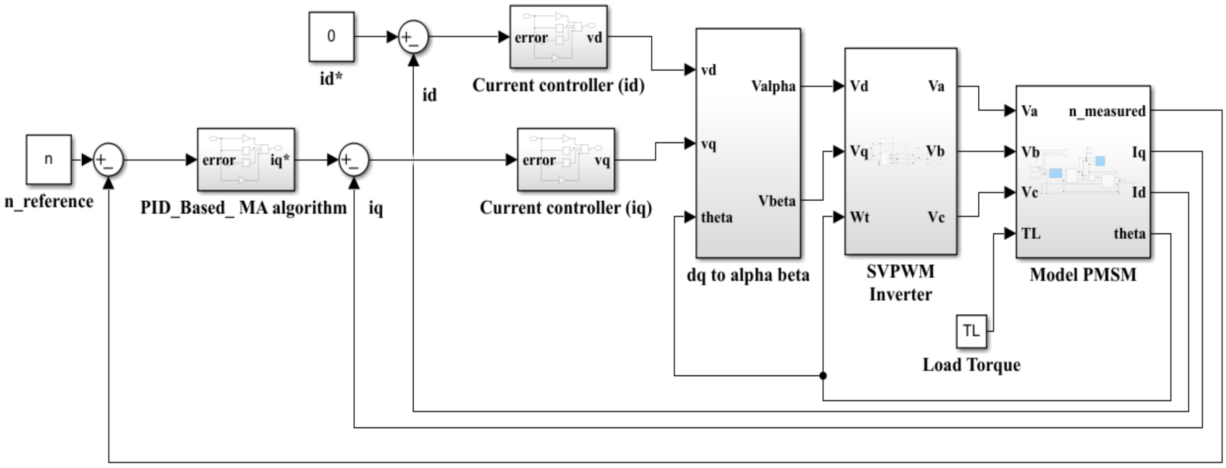

Fig. 2. The entire Simulink model for the suggested approach

3. MAYFLY ALGORITHM

A recently proposed optimization technique, the MA algorithm, models the mating and flight behavior of mayflies. It is a metaheuristic that has demonstrated efficacy in addressing optimization issues. Despite being analogous to PSO, MA is thought to have a higher ability to identify a more optimum solution than PSO, giving it a greater chance of finding the globally optimal solution. The name "Mayfly" comes from the fact that these insects are most common in the UK during May. Immature mayflies spend several years as aquatic nymphs before emerging as adult mayflies. To entice females, the majority of mature males congregate in swarms a few meters above the water's surface. They conduct a nuptial dance with distinctive up and down movements, making a pattern. Female mayflies visit these swarms to mate (Bhattacharyya et al., 2020). The population of mayflies is made up of both female and male mayflies. The ability to search locally is provided by the motions of the female and male mayflies, and the process of producing progeny through mayfly mating endows the MA with the ability to search globally (Zervoudakis and Tsafarakis, 2020, Wang et al., 2022). The mayflies emerge from their eggs, develop into aquatic nymphs, and then, when fully developed, rise to the surface. They only survive for a few days before reproducing and dying. As shown in Fig. 3, an adult mayfly must dance around a body of water to mate with a female mayfly. The female mates with the males in the air and finally drops progeny or eggs, continuing the life cycle. The male and female mayfly's dancing, movement, and mating rituals served as inspiration for the algorithm (Moosavi et al., 2021).

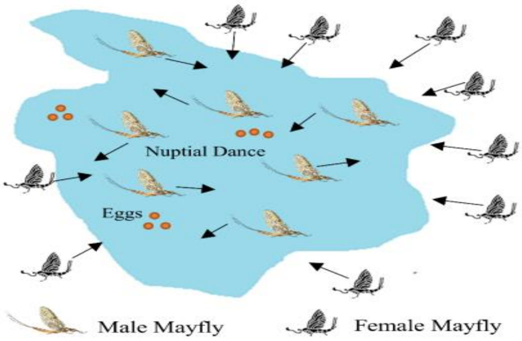

Fig. 3. Movement and mating ritual of mayflies (Moosavi et al., 2021)

a. Male Mayfly Movement

Swarms of male mayflies congregate near bodies of water. This implies that they modify their position and speed of travel based on the mayflies in their vicinity inside the swarm. Suppose x_i^t represents the mayfly's current position (i) at step time (t). The following location at a time $(t+1)$, represented via x_i^{t+1} can be expressed as follows (Moosavi et al., 2021, Mo et al., 2022):

$$x_i^{t+1} = x_i^t + v_i^{t+1} \tag{8}$$

Where v_i^{t+1} represents the mayfly velocity (i) at step time (t+1). The following rule will limit the mayflies' velocity, and their position will always stay inside the search space (x_{min}, x_{max}) (Moosavi et al., 2021, Mo et al., 2022).

$$v_i^{t+1} = \left\{\begin{array}{ll} V_{max} & if\ v_i^{t+1} > V_{max} \\ -V_{max} & if\ v_i^{t+1} < -V_{max} \end{array}\right\} \tag{9}$$

Additionally, the equation that follows provides the mayfly velocity in the swarm (Moosavi et al., 2021, Mo et al., 2022):

$$v_i^{t+1} = v_i^t + a_1 e^{-\beta r_p^2}(pbest_i - x_i^t) + a_2 e^{-\beta r_g^2}(gbest - x_i^t) \tag{10}$$

where $(a_1$ and $a_2)$ are positive constants and β is the visibility coefficient. Additionally, mayfly 'i's personal best position is represented by $pbest_i$, while the swarm's global best position is denoted by $gbest$. Only when the objective function of x_i^{t+1} is less than the objective function of $pbest_i$ is the value of $pbest_i$ updated. This is exemplified by the following expression (Moosavi et al., 2021, Mo et al., 2022):

$$pbest_i = \begin{Bmatrix} x_i^{t+1}, if\ f(x_i^{t+1} < f(pbest_i) \\ is\ kept\ the\ same, otherwise \end{Bmatrix} \tag{11}$$

Conversely, $gbest$ represents a mayfly's optimal location relative to the rest of the N mayflies in the swarm. The Cartesian distance between (x_i) and $pbest_i$ and between $(x_i\ )$and $gbest$, respectively, is defined as r_p and r_g. The distances can be determined with the following formula (Moosavi et al., 2021, Mo et al., 2022):

$$r_p\ or\ r_g = \|x_i - X_i\| = \sqrt{\sum_{j=1}^{n}\left(x_{ij} - X_{ij}\right)^2} \tag{12}$$

Where x_{ij} is the mayfly 'i''s jth element, and X_{ij} relates $to\ pbesti$ for r_p and $gbest$ for r_g. By their species' male characteristics, they engage in a nuptial dance to entice the female. For the best mayflies, this movement can be computed as follows (Moosavi et al., 2021, Mo et al., 2022):

$$v_i^{t+1} = v_i^t + d * r \tag{13}$$

Where (r) is a random number in the interval $[-1,1]$, while (d) is the nuptial dance coefficient. This adds a heuristic component to the process (Moosavi et al., 2021, Mo et al., 2022).

b. Female Mayfly Mobility

Let's indicate the female mayfly's apparent location as y_i^t. To reproduce, females don't congregate in swarms; instead, they migrate in the direction of the male. The following formula can be used to estimate the change in this position (Moosavi et al., 2021, Mo et al., 2022):

$$y_i^{t+1} = y_i^t + v_i^{t+1} \tag{14}$$

The location of the female mayfly at step time (t+1) is calculated by combining her velocity (v_i^{t+1}) to her present position. A deterministic method suggests that females and males of mayflies are attracted to each other with the same rank. Rankings are assigned based on the fitness function. Their velocities are therefore computed as shown (Moosavi et al., 2021, Mo et al., 2022):

$$v_i^{t+1} = \begin{Bmatrix} v_i^t + a_2 e^{-\beta r_{mf}^2}\left(x_i^t - y_i^t\right), & if\ f(y_i) > f(x_i) \\ v_i^t + fl * r, & if\ f(y_i) \le f(x_i) \end{Bmatrix} \tag{15}$$

Where, as stated in equation 10, a_2 and β are the same. The remoteness between the female (i) and male (i) mayflies, denoted as r_{mf}, r in the interval $[-1,1]$, and fl, a random walk coefficient (Moosavi et al., 2021, Mo et al., 2022).

c. Mating

The way a female mayfly selects her male partner for reproduction also applies to the selection of the offspring. To produce progeny, the best female mayfly mates with the best male mayfly. All mayflies, male and female, are ranked in the same way. The following equation is utilized to compute the mayfly crossover (Moosavi et al., 2021, Mo et al., 2022):

$$offspring_1 = L * x_i^t + (1 - L) * y_i^t \tag{16}$$

$$offspring_2 = L * y_i^t + (1 - L) * x_i^t \tag{17}$$

An L in equations (16) and (17) signifies an arbitrary variable falling inside a predetermined range, and y_i^t and x_i^t represent the parent female and male mayflies, respectively (Moosavi et al., 2021, Mo et al., 2022).

d. Mutation

To prevent the search of the algorithm from becoming stuck on local minima, the offspring are altered. This mutation is performed on some of the offspring mayflies via injunction of an arbitrary variable into the offspring via the equation (18) (Moosavi et al., 2021, Mo et al., 2022):

$$offspring'_n = offspring_n + \sigma\, N_n(0,1) \tag{18}$$

The standard deviation (σ) and standard normal distribution (N_n) have a mean of zero and a variance of one (Moosavi et al., 2021, Mo et al., 2022).

4. CONTROLLER DESIGN

In terms of accuracy and speed of convergence, the basic Mayfly optimization method performs superior to other swarm intelligence algorithms (Boopathi et al., 2023). This study recommends using the MA to optimize the speed controller's K_p, K_i, and K_d parameters. Fig. 4 shows the suggested speed controller of the PMSM. The MA identifies optimal PID controller values for fast PMSM response while minimizing overshoot and settling time. Fig. 5 illustrates the algorithm flow for optimizing PID parameters using MA, as discussed before. The steps are as follows (Lei et al., 2022):

A. Specify the quantity of male and female mayflies, offspring, dance coefficient, learning factor, visibility coefficient, and other parameters simultaneously. Initialize the population's locations and velocities using the parameters specified above.

B. As the optimization algorithm's fitness function, utilize the absolute error index (ITAE) of the PMSM's speed deviation and integrated time.

C. Create a simulation model of the PID speed controller of the PMSM using MATLAB's Simulink tool, as seen in Fig. 2. Next, begin entering the iteration, determine each mayfly's fitness function value, and sort the values. Additionally, as g_{best} and p_{best} are computed.

D. Use formulas to update the position and speed of female and male mayflies, as well as their mating behavior.

E. Determine the values of the variants' fitness functions and offspring's, update every individual's fitness so that it may be compared to the global fitness, and then update the global optimum.

F. Once the maximum number of iterations has been reached, terminate the process and output the outcome. If not, go back to step C and repeat the process. The ITAE can be expressed in equation 19 where (T) is the adjustment time and $e(t)$ is the system deviation:

$$J_{ITAE} = \int_0^T t\,|e(t)|dt \qquad (19)$$

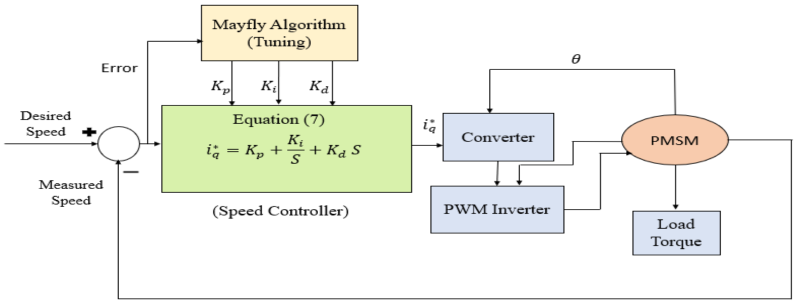

Fig. 4. Block diagram of PID-based MA speed controller of PMSM

Fig. 5 illustrates how the MA method seeks appropriate PID controller parameters. The PID controller output (i_q^*) goes to the quadrant current controller as input to compare it with the (i_q) from the PMSM.

5. RESULTS AND DISCUSSION

The suggested controller's performance is assessed through simulation in the MATLAB environment. A $3-\phi$, wye-connected motor with the parameters indicated in Table 1 serves as the permanent magnet synchronous motor model utilized in this work. To confirm the effectiveness of the suggested controller, several simulation tests for vector control of the PMSM were conducted. The proposed controller is tested under various reference speeds (250 rpm, 500 rpm, and 1500 rpm) as shown in Fig. 6, 7, and 8, respectively. To prove the efficiency of the suggested controller, the outcomes obtained were compared with the standard PSO algorithm, PSO is a method that is based on simulated bird and fish foraging behavior. It is simple to define and implement. It identifies the most likely global optimal solution for a problem. Every particle in the swarm represents a potential solution in the PSO algorithm. It is assumed that the swarm's particles travel in the search space at the corresponding velocity. Every swarm particle recalls the best location it has ever been as well as the greatest spot all particles have ever visited together. For complicated optimization issues, the standard PSO technique has limitations such as premature convergence and sluggish convergence speed (Patel and Thakker, 2016), in addition, the outcomes are also compared with the conventional PID controller. Figs. 6, 7, and 8 show that the PID-MA controller has a quicker settling time than the others, it also has less overshoot overall. PID-MA performs significantly better than the other two controllers. Also tracks the reference faster than the PID-PSO and traditional PID systems.

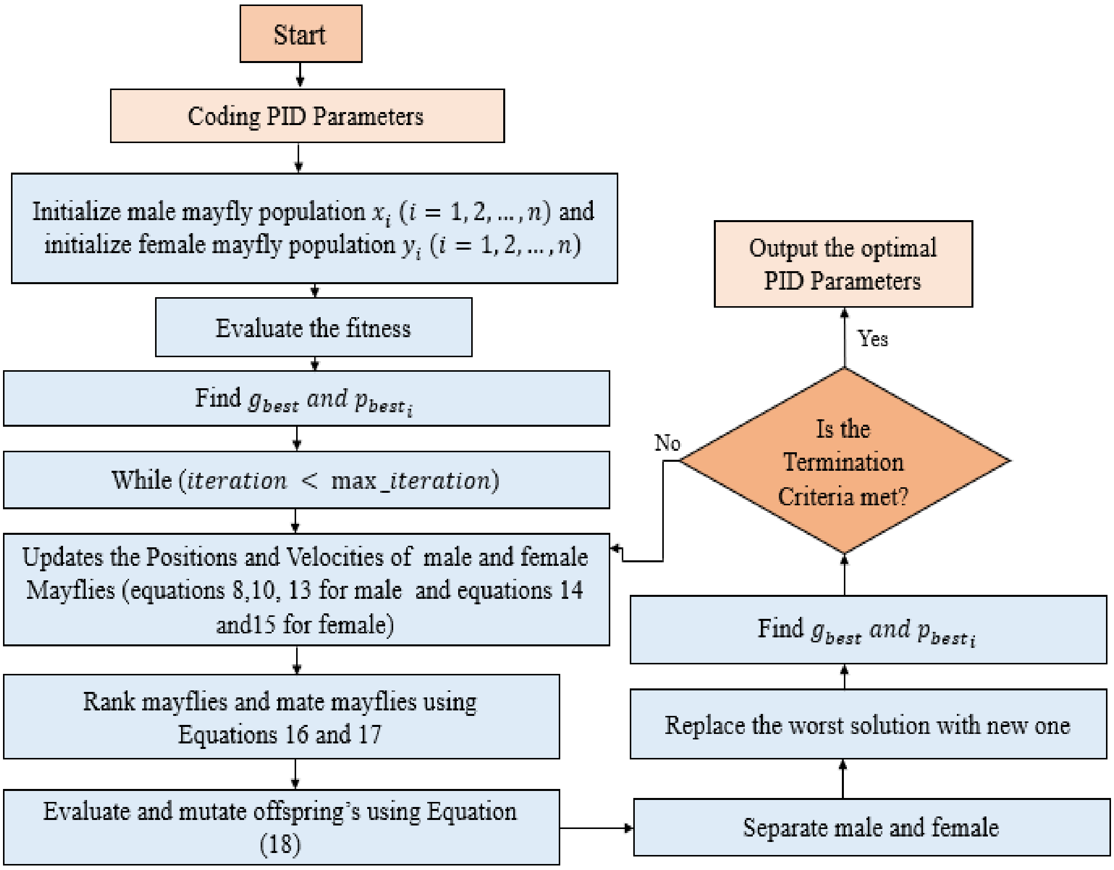

Fig. 5. Solution stages for the suggested PID depend upon the MA for the PMSM

Table 1. PMSM Parameters (Zaihidee et al., 2019)

Parameters	Value
R_S	1.2Ω
L_d	$6.35\ mH$
L_q	$6.75\ mH$
J	$2.31 * 10^{-4}\ kg\ m^2$
B	$0.0002\ Nm\ s$
λ_f	$0.15\ Wb$
P_n	4

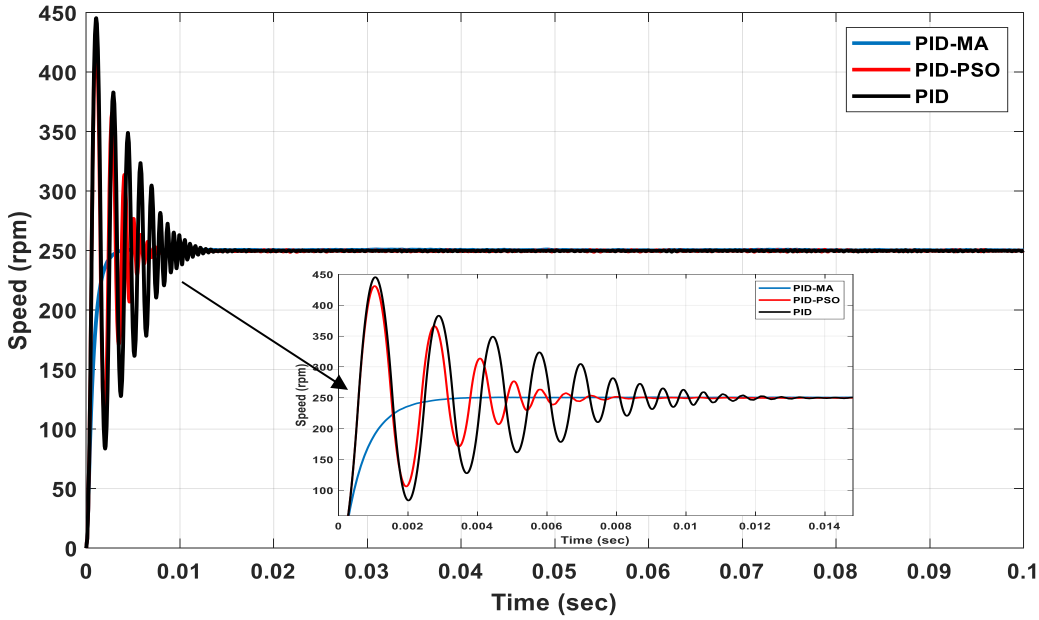

Fig. 6. Comparison of PID-MA, PID-PSO, and PID speed responses at 250 rpm as a reference speed at no load

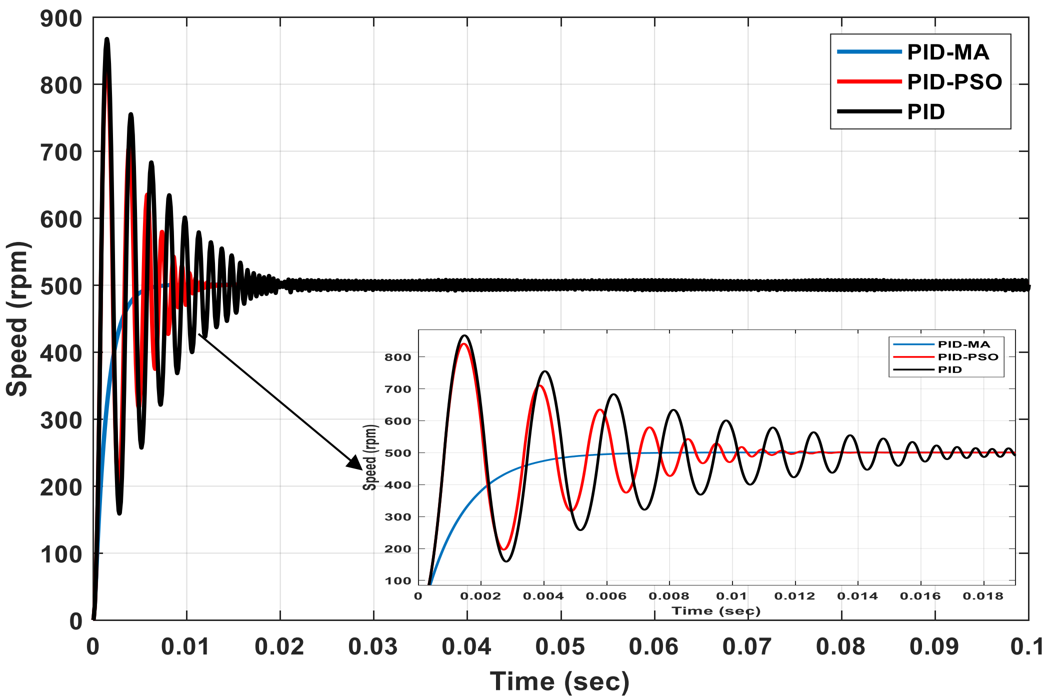

Fig. 7. Comparison of PID-MA, PID-PSO, and PID speed responses at 500 rpm as a speed reference at no load

Additionally, the speed responses to variations in the load were examined. By applying a load of 0.5 Nm at t = 0.05s, the proposed controller's disturbance rejection capabilities were assessed. Fig. 9's results demonstrate that a system driven by PID-MA performs better than PID-PSO and traditional PID systems. When a load is applied, the speed controller output (q-axis reference current) of the two controllers is compared in Fig. 10, where the PID-MA speed controller generates a reference value with less ripple. Load disturbance affects speed responses for both PID-PSO and traditional PID controllers, with PID-MA providing a superior transient response. The results clearly show that the PID-MA controller provides better overshoot and quick response times.

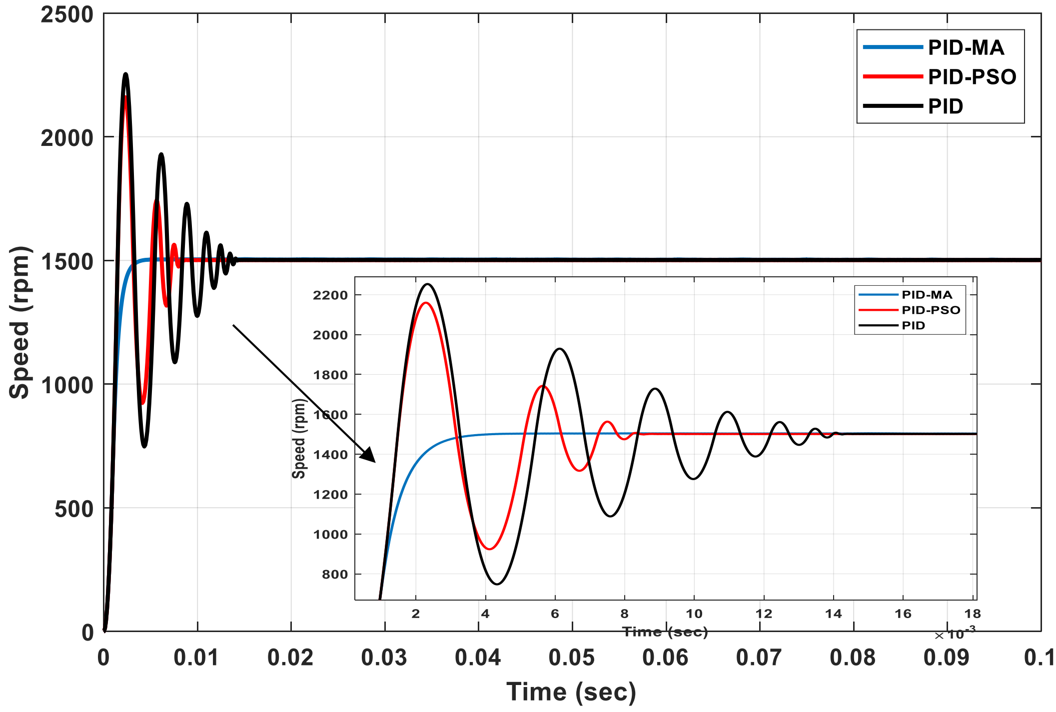

Fig. 8. Comparison of PID-MA, PID-PSO, and PID speed responses at 1500 rpm as a speed reference at no load

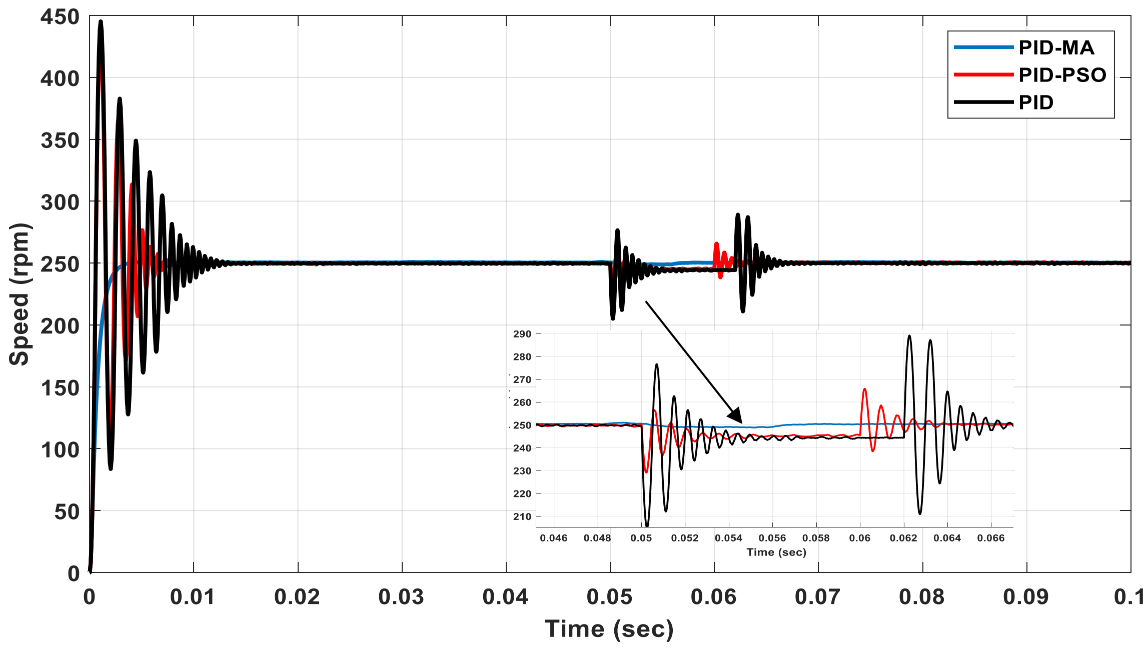

Fig. 9. Comparison of the PID-MA, PID-PSO, and PID speed drops under a 0.5 Nm load

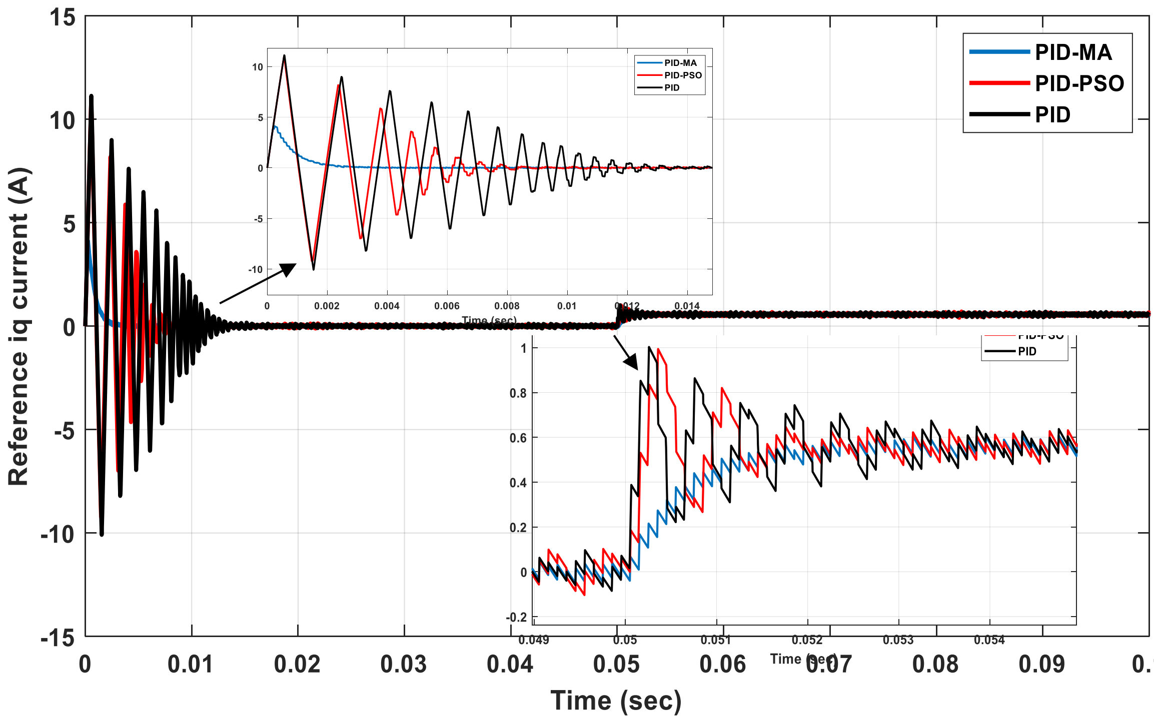

Fig. 10. Comparison of the PID-MA, PID-PSO, and PID speed controllers' q-axis reference current outputs at 0.5 Nm load

The proposed PID-MA controller's performance is further validated by applying a load of 2 N m for 0.05 seconds. Fig. 11 demonstrates the response of the speed of the suggested controller when a load of 2 Nm is applied at 0.05 sec and compared with the PID-PSO and conventional PID controllers. A comparison of the PID-MA, PID-PSO, and PID speed controllers' q-axis reference current outputs at 2 Nm load is shown in Fig. 12.

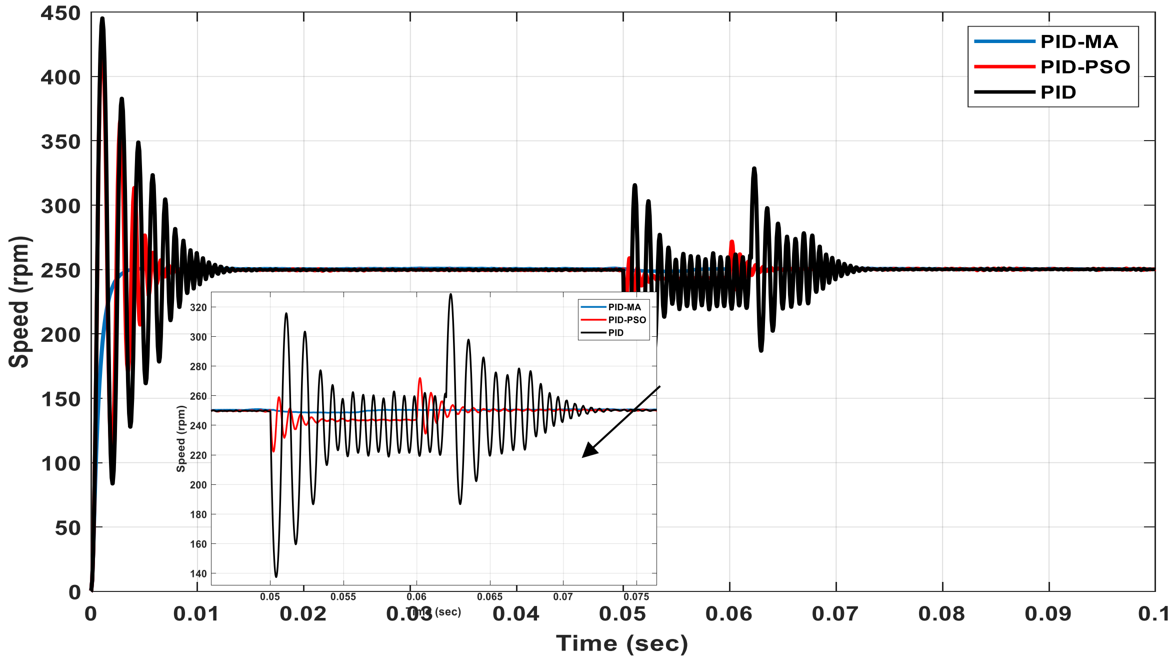

Fig. 11. Comparison of the PID-MA, PID-PSO, and PID speed drops under a 2 Nm load

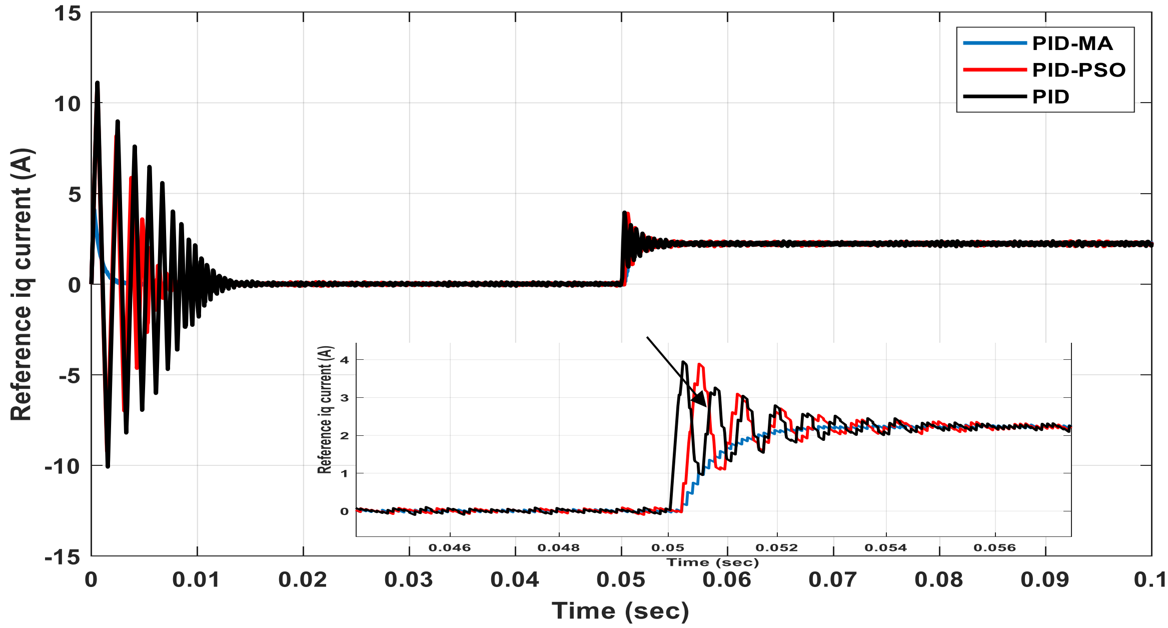

Fig. 12. Comparison of the PID-MA, PID-PSO, and PID speed controllers' q-axis reference current outputs at 2 Nm load

The response parameters for PMSM speed control for various instances are shown in Tables 2,3, and 4 respectively at a reference speed of 250 rpm, 500 rpm, and 1500 rpm at no load.

Table 2. Response parameters for PMSM speed control at reference speed 250 rpm

Approach	Overshoot	Settling time
PID-MA	0.4200	0.0027
PID-PSO	72. 5943	0.0070
PID	77.9646	0.0114

Table 3. Response parameters for PMSM speed control at reference speed 500 rpm

Approach	Overshoot	Settling time
PID-MA	0.1730	0.0052
PID-PSO	68.0733	0.0107
PID	73.2533	0.0211

Table 4. Response parameters for PMSM speed control at reference speed 1500 rpm

Approach	Overshoot	Settling time
PID-MA	0.2044	0.0029
PID-PSO	43.8655	0.0077
PID	50.0585	0.0132

6. CONCLUSION

This study discusses the speed control of permanent magnet synchronous motor drives. A PID speed controller for PMSM based on the Mayflies optimization algorithm is suggested in this study. The MA algorithm tunes the PID controller to attain a reference speed or compensate for load torque disturbances while maintaining a constant rotational speed. To confirm the efficacy of the recommended method, three different speed conditions high, medium, and low speed as well as the addition of a load disturbance to the motor during operation were used in the simulations. The PID-based PSO and conventional PID controller were also tested under the same circumstances as the suggested controller for comparison's sake. The simulation outcomes show that the PID-based MA control system can improve the motor's running performance at low, medium, and high speeds. In terms of speed, overshoot is significantly decreased, and the load can be returned promptly after loading. In the interim, the controller exhibits excellent resilience against the disturbance and good transient responsiveness.

7. REFERENCES

AHMED, Y., HOBALLAH, A., HENDAWI, E., AL OTAIBI, S., ELSAYED, S. K. & ELKALASHY, N. I. 2021. Fractional order PID controller adaptation for PMSM drive using hybrid grey wolf optimization. International Journal of Power Electronics and Drive Systems, 12, 745.

AMUDHA, M., RAMACHANDRAN, M., SIVAJI, C. & GAYATHRI, R. 2021. A Study on Climate Change with Mayfly Algorithm Optimization. Recent trends in Management and Commerce, 2, 23-28.

BHATTACHARYYA, T., CHATTERJEE, B., SINGH, P. K., YOON, J. H., GEEM, Z. W. & SARKAR, R. 2020. Mayfly in harmony: A new hybrid meta-heuristic feature selection algorithm. IEEE Access, 8, 195929-195945.

BOOPATHI, D., JAGATHEESAN, K., ANAND, B., SAMANTA, S. & DEY, N. 2023. Frequency regulation of interlinked microgrid system using mayfly algorithm-based PID controller. Sustainability, 15, 8829.

CERVONE, A., DORDEVIC, O. & BRANDO, G. 2021. General approach for modeling and control of multiphase PMSM drives. IEEE Transactions on Power Electronics, 36, 10490-10503.

CHEN, H., WANG, X., BENBOUZID, M., CHARPENTIER, J.-F., AÏT-AHMED, N. & HAN, J. 2022. Improved Fractional-Order PID Controller of a PMSM-Based Wave Compensation System for Offshore Ship Cranes. Journal of Marine Science and Engineering, 10, 1238.

DENG, Y., WANG, J., LI, H., LIU, J. & TIAN, D. 2019. Adaptive sliding mode current control with sliding mode disturbance observer for PMSM drives. ISA transactions, 88, 113-126.

GUO, T., CHEN, Y., CHEN, Q., LIN, T. & REN, H. 2022. An IPMSM Control Structure Based on a Model Reference Adaptive Algorithm. Machines, 10, 575.

HUANG, S., GUO, X., WANG, R. & MEI, Y. 2021. A SVPWM algorithm based on four-switch three-phase inverter for PMSM under the imbalance of bus capacitor voltage. Journal of Power Electronics, 21, 1812-1822.

INJETI, S. K. & DIVYAVATHI, M. 2019. Optimal Gain Scheduling of PID Controller for the Speed Control of PMSM Drive Using Bio-Inspired Optimization Algorithms. International Journal on Electrical Engineering & Informatics, 11.

JAMIL, I. A. A. & MOGHAVVEMI, M. Optimization of pid controller tuning method using evolutionary algorithms. 2021 Innovations in Power and Advanced Computing Technologies (i-PACT), 2021. IEEE, 1-7.

JIN, F., WAN, H., HUANG, Z. & GU, M. PMSM vector control based on fuzzy PID controller. Journal of Physics: Conference Series, 2020. IOP Publishing, 012016.

JUNEJO, A. K., XU, W., MU, C., ISMAIL, M. M. & LIU, Y. 2020. Adaptive speed control of PMSM drive system based a new sliding-mode reaching law. IEEE Transactions on Power Electronics, 35, 12110-12121.

LEI, G., CHANG, X., TIANHANG, Y. & TUERXUN, W. 2022. An improved mayfly optimization algorithm based on median position and its application in the optimization of PID parameters of hydro-turbine governor. IEEE Access, 10, 36335-36349.

LIANG, W., WANG, J., LUK, P. C.-K., FANG, W. & FEI, W. 2014. Analytical modeling of current harmonic components in PMSM drive with voltage-source inverter by SVPWM technique. IEEE Transactions on Energy Conversion, 29, 673-680.

LIN, X., HUANG, W. & WANG, L. 2018. SVPWM strategy based on the hysteresis controller of zero-sequence current for three-phase open-end winding PMSM. IEEE Transactions on Power Electronics, 34, 3474-3486.

LIU, H., LIN, W., LIU, Z., BUCCELLA, C. & CECATI, C. 2022. Model predictive current control with model-aid extended state observer compensation for PMSM drive. IEEE Transactions on Power Electronics, 38, 3152-3162.

MO, S., YE, Q., JIANG, K., MO, X. & SHEN, G. 2022. An improved MPPT method for photovoltaic systems based on mayfly optimization algorithm. Energy Reports, 8, 141-150.

MOOSAVI, S. K. R., ZAFAR, M. H., AKHTER, M. N., HADI, S. F., KHAN, N. M. & SANFILIPPO, F. A novel artificial neural network (ANN) using the mayfly algorithm for classification. 2021 International Conference on Digital Futures and Transformative Technologies (ICoDT2), 2021. IEEE, 1-6.

ORLOWSKA-KOWALSKA, T., WOLKIEWICZ, M., PIETRZAK, P., SKOWRON, M., EWERT, P., TARCHALA, G., KRZYSZTOFIAK, M. & KOWALSKI, C. T. 2022. Fault diagnosis and fault-tolerant control of PMSM drives–state of the art and future challenges. IEEE Access, 10, 59979-60024.

ORTEGA, R., ASTOLFI, A. & BARABANOV, N. E. 2002. Nonlinear PI control of uncertain systems: an alternative to parameter adaptation. Systems & control letters, 47, 259-278.

PATEL, S. & THAKKER, R. A. 2016. Automatic Circuit Design and Optimization Using Modified PSO Algorithm. Journal of Engineering Science & Technology Review, 9.

REN, N., FAN, L. & ZHANG, Z. 2021. Sensorless PMSM control with sliding mode observer based on sigmoid function. Journal of Electrical Engineering & Technology, 16, 933-939.

SUN, X., LI, T., YAO, M., LEI, G., GUO, Y. & ZHU, J. 2021. Improved finite-control-set model predictive control with virtual vectors for PMSHM drives. IEEE Transactions on Energy Conversion, 37, 1885-1894.

SUN, X., LI, T., ZHU, Z., LEI, G., GUO, Y. & ZHU, J. 2021. Speed sensorless model predictive current control based on finite position set for PMSHM drives. IEEE Transactions on Transportation Electrification, 7, 2743-2752.

TEYMOORI, V., ARISH, N., MORADI, M. & GHALEBANI, P. 2023. Permanent Magnet Synchronous Motor (PMSM) Speed Response Correction Using Fuzzy-PID Self-Tuning Controller Under Sudden and Gradual Load Variation. International Journal of Systems Engineering, 6, 46-58.

THIKE, R. & PILLAY, P. 2020. Mathematical model of an interior PMSM with aligned magnet and reluctance torques. IEEE Transactions on Transportation Electrification, 6, 647-658.

WANG, F., ZUO, K., TAO, P. & RODRÍGUEZ, J. 2020. High performance model predictive control for PMSM by using stator current mathematical model self-regulation technique. IEEE Transactions on Power Electronics, 35, 13652-13662.

WANG, X., PAN, J.-S., YANG, Q., KONG, L., SNÁŠEL, V. & CHU, S.-C. 2022. Modified mayfly algorithm for UAV path planning. Drones, 6, 134.

WU, T., ZHOU, C., YAN, Z., PENG, H. & WU, L. 2020. Application of PID optimization control strategy based on particle swarm optimization (PSO) for battery charging system. International Journal of Low-Carbon Technologies, 15, 528-535.

ZAIHIDEE, F. M., MEKHILEF, S. & MUBIN, M. 2019. Application of fractional order sliding mode control for speed control of permanent magnet synchronous motor. Ieee Access, 7, 101765-101774.

ZERVOUDAKIS, K. & TSAFARAKIS, S. 2020. A mayfly optimization algorithm. Computers & Industrial Engineering, 145, 106559.

ZHANG, Y., JIANG, H. & YANG, H. 2020. Model predictive control of PMSM drives based on general discrete space vector modulation. IEEE Transactions on Energy Conversion, 36, 1300-1307.